

Thermal Program Desorption Mass Spectrometry of PAHs from Mineral and Organic Surfaces

Jeffrey W. Talley,^{1,*} Upal Ghosh,² John S. Furey,³ Samuel G. Tucker,⁴
and Richard G. Luthy⁵

¹*Department of Civil Engineering and Geological Sciences
University of Notre Dame
Notre Dame, IN 46556*

²*Department of Civil and Environmental Engineering
University of Maryland Baltimore County
Baltimore, MD 21250*

³*DynCorp
Vicksburg, MS 39180*

⁴*Environmental Laboratory
U.S. Army Engineer Research and Development Center (ERDC)
Vicksburg, MS 39180*

⁵*Department of Civil and Environmental Engineering
Stanford University
Stanford, CA 94305-4020*

ABSTRACT

This research investigated the release of polycyclic aromatic hydrocarbons (PAHs) from spiked materials using thermal desorption mass spectrometry. Experimental methods were developed to obtain real-time PAH desorption data through use of a thermal program desorption probe. Data analysis techniques were investigated to explore the thermal desorption profiles of milligram-size samples. Peak temperatures of desorption were observed to vary among PAHs and among sorbents. For the same absorbent, peak temperatures increased with an increase of PAH molecular weights. For the same PAH, peak temperatures increased as the sorbent varied from sand to alumina to XAD-4 to kaolin. These results have been interpreted in terms of a combined model that include both an activation energy and a desorption/volatilization rate coefficient.

Key words: thermal program desorption; mass spectrometry; PAHs; mineral; surface chemistry

*Corresponding author: Department of Civil Engineering and Geological Sciences, University of Notre Dame, Notre Dame, IN 46556. Phone: 574-631-5164; Fax: 574-631-9256; E-mail: jtalley1@nd.edu

INTRODUCTION

POLYCYCLIC AROMATIC HYDROCARBONS (PAHs) preferentially bind to various components of soil and sediment, depending on organic matter content and type (Ghosh *et al.*, 2000; Karapanagiota *et al.*, 2000). The degree of PAH binding with geosorbents strongly influences PAH availability and environmental effects. For example, a major factor influencing successful sediment bioremediation is the availability of contaminants to micro-organisms for degradation, whereas contaminants that are strongly sorbed and not available to micro-organisms may also not be available for a toxic response. Thus, an understanding of how binding to a solid substrate changes the availability of PAHs is important for evaluating the environmental fate and effects of these compounds. The processes affecting the availability of PAHs sequestered in soil and sediment are complex due to the large heterogeneity in soil/sediment particle types and sorbent organic matter typically present (Luthy *et al.*, 1997).

The availability of a compound sorbed on a solid surface can be described by the escaping tendency as quantified by fugacity. For a pure compound with equilibrated phases, the fugacity is the same as the vapor pressure. However, when a compound sorbs on a surface, the binding with the substrate results in a reduction of the fugacity. Thus, the vapor pressure of a compound sorbed to a solid material can provide an indication of the binding and relative availability of the compound. For many environmentally significant hydrophobic organic compounds (HOCs) like PAHs the vapor pressure at ambient temperatures are very low and difficult to measure directly. Because vapor pressure increases rapidly with temperature, many methods invoke higher temperatures for measuring vapor pressure or release of high molecular weight organic compounds from surfaces.

Various adaptations of thermal program desorption (TPD) techniques have been used in the past to study: desorption of gases from solid surfaces (Falconer and Madix, 1975; King, 1975), desorption of toluene from kaolin pellets (Keys and Silcox, 1994), pyrolysis of hydrocarbons from coal (Yun and Meuzelaar, 1991), estimation of PAH vapor pressures (Oja and Suuberg, 1997; Tesconi and Yalkowski, 1998), and desorption activation energies of trichloroethylene from silica gel (Farrell *et al.*, 1999). Thermal desorption techniques have also been explored for their utility in detecting and quantifying organic contaminants in soil samples (Robbat *et al.*, 1992). Unlike other techniques for soil analysis, TPD requires no solvent extraction, little sample preparation, and is relatively quick. Samples are heated inside an oven or thermal desorption probe (which can hold a small sample vial at the tip, and be inserted into a mass spectrometer), and

as the temperature increases the volatilized compounds are collected and detected by the mass spectrometer. The use of a direct insertion probe, which does not require transfer lines, with a mass spectrometer (MS) can allow measurement of the release of trace organics from very small samples. Direct probes have been used for the analysis of coal pyrolysis products by Yun and Meuzelaar (1991). To date, thermal desorption mass spectrometry with direct probes has been used for study of pyrolysis and as a means for inserting a sample into a mass spectrometer for compound identification.

The primary objectives of this work were to study the release characteristics of PAHs sorbed on different mineral and organic surfaces (glass, sand, kaolin, alumina, XAD-4 resin beads, and pulverized activated carbon) by using thermal program desorption mass spectrometry with a direct insertion probe, and to explore the simulation of the TPD profiles of PAHs in terms of a combined model that include both an activation energy and a desorption/volatilization rate coefficient.

MATERIALS AND METHODS

Instrumentation

A schematic of the TPD-MS used in this work is shown in Fig. 1. The probe used was a Thermoquest GCQ *Plus* Direct Insertion Probe with a glass sample vial, as shown in Fig. 2. This instrument configuration was selected so that a sample could be inserted directly into the ion volume of the MS. This allowed for better transfer of desorbed compounds as well as increased sensitivity. The sample is emplaced in an open sample vial and weighed. The sample vials are cylindrical with an inside diameter of 1.0 by 10-mm length. The probe holding the vial is inserted into the MS and heated linearly. The ion trap in

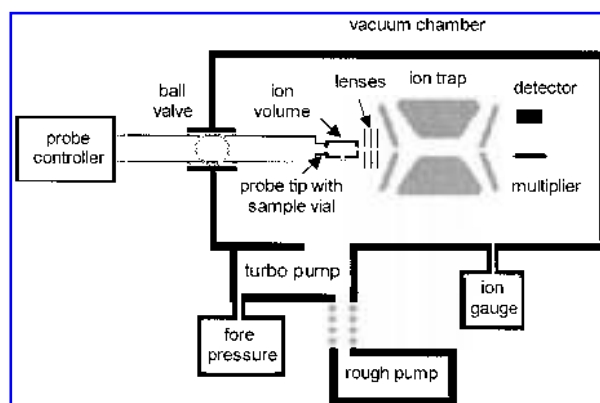


Figure 1. Schematic of thermal program desorption mass spectrometer with a direct insertion probe.

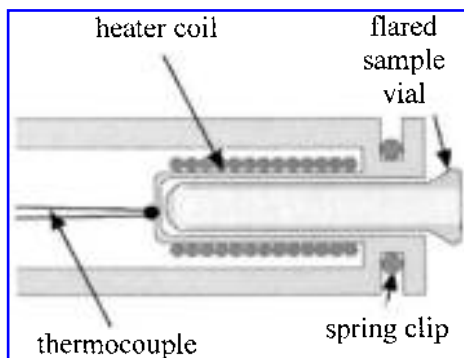


Figure 2. Schematic of direct insertion probe tip with a sample vial placed inside.

the TPD-MS is a chamber consisting of an ion source, injection optics, quadrupole mass analyzer, multiplier, and detector. The system is filled with helium damping gas, and is regulated so that pressure in the system is approximately 10^{-7} atm. Voltage is applied within the ion source and the excited ions produced by electron impact are then projected sequentially through a series of lenses to the mass analyzer. The cycle time for the entire process is in the range of milliseconds.

Within each TPD run, the raw ion count is proportional to the molecular flux in the ion volume. Thus, the ion count measured at any time is proportional to the rate of release of PAHs from the sample vial. PAHs typically produce molecular ions with little fragmentation ($M + e^- \rightarrow M^+ + 2e^-$), allowing multiple compounds to be analyzed simultaneously provided they have different molecular weights. The PAH mass homologs used in this work are shown in Table 1. The sensitivity of the instrument with the direct insertion probe accommodates very small samples and in our work down to the single particle scale for granular material (0.1-mm diameter). The sample amount was small enough so that no retardation due to interparticle sorption was observed (Ghosh *et al.*, 2001).

Method development

A primary task in this research was to provide an efficient and concise protocol for TPD-MS operation. The variables tested included sample vial configuration, sample volume, temperature ramp rates of 10°C , 20°C , or 30°C per minute, and final temperatures. A heating ramp rate of $10^\circ\text{C}/\text{min}$, final temperature of 400°C , and no hold time were selected. The temperature ramp rate of $10^\circ\text{C}/\text{min}$ was chosen because of consistency and the ability to distinguish the different PAH homologs. A higher temperature ramp rate did not allow time for the PAH molecular weight 178 (phenanthrene and anthracene) to show a desorption curve on a consistent ba-

sis with some of the materials tested. A shift toward higher peak temperatures for desorption response with increased heating rate has been described by Yun and Meuzelaar (1991). In that case, the PAH could be released at a slightly elevated temperature because there maybe insufficient time for temperature equilibration. We observed through full-scan MS spectrum that many organic samples exhibited pyrolysis starting at approximately 400°C , except for some coals, which showed pyrolysis beginning at around 250°C . Our aim was to note when pyrolysis occurs and to avoid those conditions, if possible. Thus, to make the desorption as complete as possible with uniformity, a maximum temperature of 400°C was chosen for all runs reported here. Stopping a run at a lower temperature would prevent the heavier molecular weight PAHs (276 and 278) from desorbing completely for some materials.

The effect of the volume and size of solid material in the vial was investigated to assess the concomitant effects of packing on TPD response. All powdery samples exhibited a volume-dependent TPD response that was attributed to interparticle diffusion, such as illustrated in Fig. 3. In these runs Ottawa sand was spiked with 40 ppm of MW 228 homolog (benzo[a]anthracene and chrysene) and 1.8 mg sand (3 grains) were placed in the vial. The sand grains were then covered with 0, 3, or 6 mm of kaolin. The results show that mass diffusion through the kaolin delayed the TPD-MS response. No similar effect was seen for any coarse mineral samples, which points to an interparticle diffusion delay for fine grained material packed in the sample vial.

Tests were run with materials spiked with PAHs to assess the extent to which diffusion mass transport may restrict the release of PAHs from kaolin. In these tests the sample vial was filled with material at various levels to assess the conditions for which the release of the PAH was independent of the amount of material in the sample vial. Hundreds of TPD runs were performed on sizes

Table 1. PAH compounds in spike standard mixture.

Mass homolog	Compounds
128	naphthalene
152	acenaphthylene
154	acenaphthene
178	phenanthrene, anthracene
202	fluoranthene, pyrene
228	benzo[a]anthracene, chrysene
252	benzo[b]fluoranthene, benzo(k)fluoranthene, benzo[a]pyrene
276	benzo[g,h,i]perylene, indeno(1,2,3-c,d)pyrene
278	dibenzo[a,h]anthracene

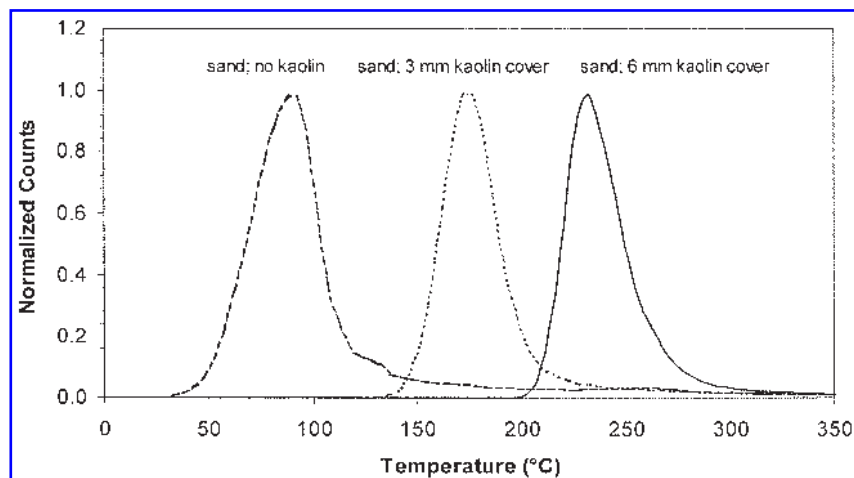


Figure 3. Thermal program desorption mass spectrometry response for PAH mass 228 homolog for PAH spiked sand covered by clean kaolin. Left curve is with no kaolin, middle curve is with 3 mm of kaolin covering the sand, and right curve is with 6 mm of kaolin covering the sand.

ranging from individual particles up to full sample vials. It was demonstrated that the smaller sample sizes of 1/8 and 1/16 filled sample vials were optimum, especially for powdery samples. Specifically, we observe a longer tailing of the TPD-MS curve for samples with sizes greater than 1/8 filled vials. From this observation, we inferred that “interparticle-diffusion” was influencing or retarding the movement of PAHs out of the sample vial. Therefore, all TPD analysis presented here used a 1/8 filled sample vial.

Materials

Various surrogate surfaces were studied during method development, and results for seven are reported in this work: kaolin, pulverized activated carbon, glass beads, XAD-4 resin, alumina, and sand. The kaolin was bulk powder (Aldrich Chemical Co., Inc., Milwaukee, WI, cat. #228834), the pulverized activated carbon was BL pulverized from Calgon Carbon Corporation (Columbus, OH), the sand was washed Ottawa sand, 20–30 mesh with typical dimension of about 400 μm (Fisher, Fairlane, NJ, cat. #S23-3), the glass beads (Biospec Products, Inc., Bartlesville, OK; cat. #11079-105) with a nominal diameter of 0.5 mm, XAD-4 resin beads were (Aldrich Chemical Co., Inc.; cat. #37380-42-0), and alumina (Scientific Instrument Services, Inc., Ringoes, NJ; cat. #ALX6004, 600 grit). The specific areas using BET nitrogen test for sand, alumina, XAD-4, and kaolin are 0.01, 3.7, 760, and 23 m^2/g , respectively. PAH standards were prepared from a PAH mixture (Sigma, St. Louis, MO; cat. #4-7930) of 16 PAHs (listed in Table 1) in dichloromethane (Sigma; cat. #AH 300-4). The dichloromethane used was HPLC grade, methanol was GC grade, and the water was distilled deionized.

Spiking procedure

An initial series of tests were conducted with individual PAH compounds spiked directly into the TPD sample vial followed by tests with the mixture of 16 EPA priority pollutant PAHs spiked either into the TPD sample vial or onto various solids. The PAH molecular weights in the mixture are shown in Table 1, and PAH compounds within a homolog were not analyzed separately. Clean sample surfaces were prepared by washing first in water and then methanol, with thorough drying in ambient room air. Homogenization was achieved by manual stirring. The solid surfaces were spiked at several concentrations, with 20 ppm concentration each per PAH reported for most test in this work, which for the 16 compounds corresponds to 320 ppm total PAHs. One gram of solid sample was saturated with dichloromethane to produce a slurry. For the 20-ppm PAH mixture, 50 μL of a 1 to 5 dilution of the 2000 mg/L PAH standard in dichloromethane was spiked into the slurry, and stirred continuously for 15 min, followed by 5-min stirring every hour for 4 h. Between the stirs, the material was allowed to dry in ambient air. Samples were stored in glass containers with foil-lined tops in a dark cooler at 4°C. Results reported in this work are average of triplicate runs measured the same day as spiking.

RESULTS AND DISCUSSION

TPD response of PAHs from glass

In tests with individual PAHs, 1 μL 100 ng/ μL of a PAH in dichloromethane was added into the empty glass TPD sample vial and allowed to evaporate for 15 min-

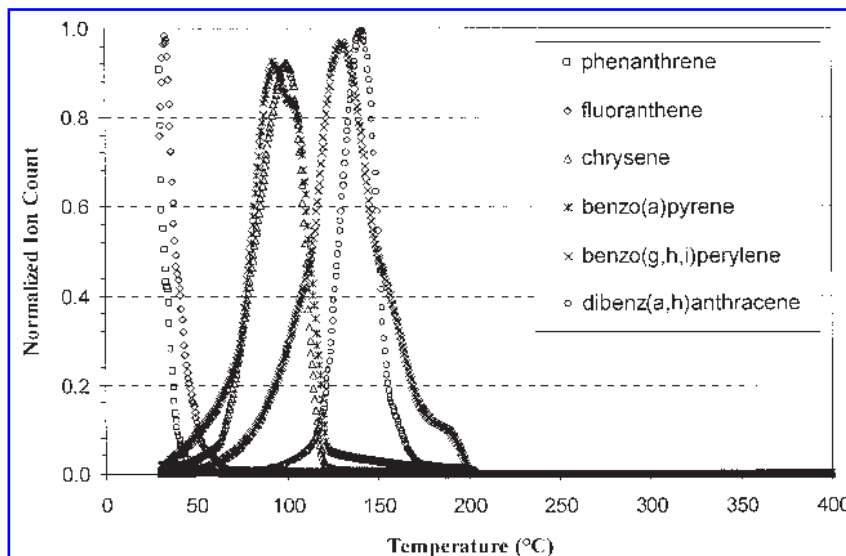


Figure 4. Thermal program desorption mass spectrometry profiles for individual PAHs spiked separately into an empty sample vial.

utes before the start of the run. A visible residue after evaporation indicated crystallization of solid PAH compounds within the vial. Results of TPD-MS analysis of a PAH-spiked sample vial is shown in Fig. 4 for tests with six PAHs. These data show the release of phenanthrene and fluoranthene at 30°C at the start of the run owing to the low pressure in the instrument. The other four PAHs show release at peak temperatures of 102, 106, 130, and

143°C, increasing with the molecular weight of the PAH compounds. To visually compare the TPD responses, the data were normalized by dividing by the total area under the peak of the TPD response curve (for Figs. 4, 5, and 6).

Data in Fig. 5 show results for release of PAHs from the mixture of 16 compounds spiked into an empty sample vial. One microliter of the mixture of 16 PAHs each at 500 ng/μL was transferred into the empty glass TPD

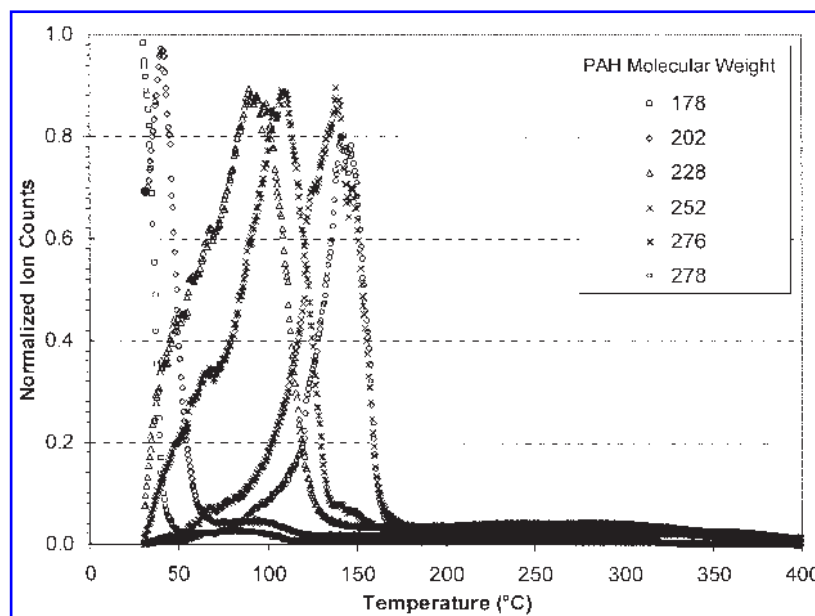


Figure 5. Thermal program desorption mass spectrometry profile for a mixture of 16 PAHs spiked into an empty sample vial.

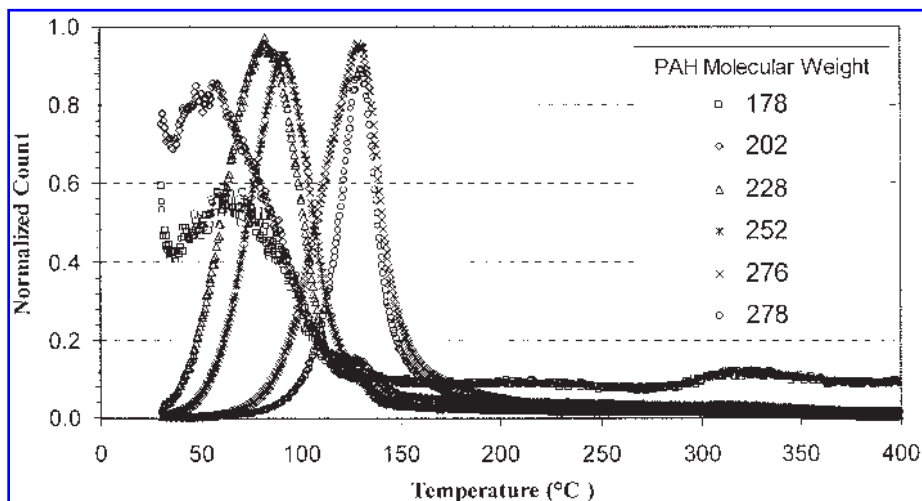


Figure 6. Thermal program desorption mass spectrometry profile for a mixture of 16 PAHs spiked onto glass beads.

sample vial and allowed to evaporate for 15 min before the start of the run. Comparison of the results of the TPD-MS data in Figs. 4 and 5 shows broader peaks for the mixtures but otherwise little difference in the appearance of the PAH peaks when added to the vial as individual PAHs or added as a mixture of 16 PAHs. Thus, the TPD response of a solid PAH is not affected significantly by the presence of other PAHs as a solid mixture.

Results in Fig. 6 show the release of PAHs from glass beads. As in the case of PAHs spiked directly in the glass sample vial, the release of PAHs from glass beads coated with PAHs shows a similar increase in peak temperature with increasing molecular weight. Molecular weights 276 for the sample vial, and 178 and 202 for glass beads show a split peak, which may be indicative of different desorption responses for the two PAH compounds comprising the mass homologs. The release of PAHs from the spiked sample vial and PAH-coated glass beads are expected to be characteristic of volatilization of solid PAHs from a noninteracting surface, which may be described semi-quantitatively by the increase in vapor pressure with temperature of these compounds.

TPD peak response for solid PAHs from vapor pressure estimation

The tendency of a condensed pure chemical to transfer into a gaseous environmental phase is determined by its vapor pressure. For most organic compounds, whether liquid or solid, the vapor pressure increases rapidly with temperature. At the boiling point, the vapor pressure equals the ambient pressure and the compound is rapidly converted to the gaseous form. In the TPD ion chamber, the ambient pressure was on the order of 10^{-7} atm. Thus,

knowledge of how the vapor pressure of PAHs changes with temperature may provide an indication of the temperature at which the maximum rate of PAH release may be observed in a TPD experiment comprising solid PAHs.

The vapor pressure of an organic liquid can be estimated theoretically from Equation (1), which is derived from the Clausius-Claperyon equation (Mackay *et al.*, 1982; Schwarzenbach *et al.*, 1993).

$$\ln P^o = 19 \left(1 - \frac{T_b}{T} \right) + 8.5 \left(\ln \frac{T_b}{T} \right) \quad (\text{atm}) \quad (1)$$

where P^o is the vapor pressure of the compound [atm], T_b is the boiling point of the compound [K], and T is the temperature [K] for which the vapor pressure is being estimated. Below the melting point of a compound, Equation (1) yields the vapor pressure of the subcooled liquid denoted as $P^o(L)$. An approximate relationship between the solid vapor pressure $P^o(s)$ and $P^o(L)$ is given by Prausnitz (1969):

$$\ln \frac{P^o(s)}{P^o(L)} = - \frac{\Delta S_{\text{melt}}(T_m)}{R} \left(\frac{T_m}{T} - 1 \right) \quad (2)$$

where $\Delta S_{\text{melt}}(T_m)$ [J/mol-K] is the entropy of fusion at the melting point, and R is the gas constant. Using Equations (1) and (2), the vapor pressure of an organic compound from its solid or liquid state can be estimated from entropy of fusion, melting point, and boiling point. The relevant thermodynamic data of eight representative PAHs were obtained from the NIST database (<http://webbook.nist.gov/chemistry/>) and Mackay *et al.* (1992).

These estimated vapor pressures of the eight representative PAH compounds are plotted in Fig. 7. Measured values of vapor pressures for naphthalene, fluorene, and phenanthrene CRC (Weast, 1985) are shown also in Fig. 7 for confirmation for these calculations. It is seen that the

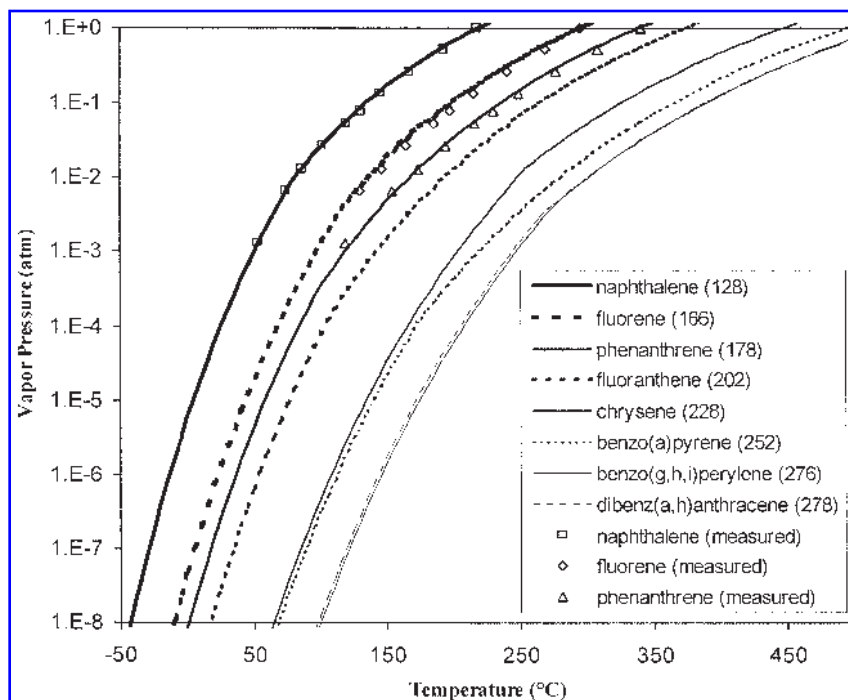


Figure 7. Change in vapor pressure with temperature for eight representative PAHs.

estimated vapor pressures match closely with the experimentally measured values. During the TPD experiments, the increasing temperature initially produces an increasing flux of PAHs into the ion chamber. After the quantity of PAHs in the sample becomes depleted, the PAH flux into the ion chamber decreases as the temperature is increased further. The maximum flux was observed to be near the temperature at which the estimated vapor pressure of the PAHs equals the ion chamber pressure.

During the TPD experiments, the pressure within the ion chamber of the mass spectrometer was measured to be 1.4×10^{-7} to 2.2×10^{-7} atm. Data in Table 2 compares the observed peak temperatures with the temperatures at which the estimated vapor pressure of the PAHs equals the pressure within the TPD instrument, for individual PAHs and PAH homologs in a mixture spiked into a sample vial and on glass beads. These estimated temperatures for naphthalene, fluorene, and phenanthrene are lower than the starting temperature of the TPD experiment. Desorption peaks for naphthalene and fluorene were not observed in the TPD experiments where the sample vial or glass beads were spiked with 16 PAH compounds. For phenanthrene and fluoranthene, the latter part of the TPD desorption peak was observed, as shown in Figs. 4–6. The peak temperatures of desorption of the remaining four listed PAHs for the spiked sample vial and the glass beads are near the temperatures for which the estimated vapor pressure equals the ion chamber pressure of 10^{-7} atm. Thus, the release of PAHs de-

posited on glass surfaces is similar to what is expected from a pure solid PAH based on estimate of vapor pressure increase with temperature. The pure solid-like desorption behavior for PAHs deposited on these glass surfaces is expected due to the low surface area and low binding affinity for PAHs on glass.

TPD-MS response of PAHs sorbed on geologic materials

PAHs were spiked on sand, kaolin, and alumina to study how the binding of PAHs on these materials affect thermal desorption. The polymeric resin XAD-4 and pulverized activated carbon were studied as surrogates for polymeric organic matter and soot carbon, respectively, that may be found in soils and sediments. Three TPD profiles of PAH molecular weight 252 spiked on sand (60 ppm) and the average response is shown in Fig. 8 to illustrate the reproducibility of the desorption response of PAHs from these natural materials. The average peak temperature (T_p) for the three runs is 108°C . There is little difference in the peak temperature between replicates of 1/8 filled sample vials for molecular weight 252 on spiked sand or for the other molecular weights (data not shown). There was a difference in the absolute peak height of the TPD response between replicates. This was probably a result of heterogeneity of PAH concentrations at the sample scale, which was of the order of a mil-

Table 2. Temperature data for PAHs.

PAH compound or homolog	Melting point (°C)	Boiling point (°C)	VP = 10 ⁻⁷ atm (°C)	T _p , spiked vial, single PAH (°C)	T _p , spiked vial, 16 PAH mix (°C)	T _p , glass beads, 16 PAH mix (°C)
naphthalene (128)	81	218	-29	NA ^a	NA	NA
fluorene (166)	116	295	5	NA	NA	NA
phenanthrene (178)	99	339	18	NA	NA	NA
fluoranthene (202)	110	375	34	33	41	49
chrysene (228)	255	448	85	102	94	81
benzo[a]pyrene (252)	177	495	88	106	111	92
benzo[g,h,i]perylene (276)	277	525	121	130	136	130
dibenzo[a,h]anthracene (278)	266	524	119	143	148	131

Melting points and boiling points, estimated temperature at which vapor pressure = 10⁻⁷ atm, and observed peak desorption temperature (T_p) for individual PAHs and PAH homolog spiked either to the sample vial or glass beads.

^aNA, not available.

ligram, as well as the semiquantitative nature of this direct probe method.

Each of the solid surfaces exhibited a similar trend for TPD response in regard to the relationship of peak temperature and PAH molecular weight. As shown in Fig. 9, an increase in peak temperature was associated with an increase in PAH molecular weight. PAH molecular weight 276 and 278 are not sufficiently different in boiling point to exhibit markedly different peak temperatures. The sample vial with individual PAHs and the sample vial with the 16 PAH mixture, and glass beads, and sand spiked with the 16 PAH mixture, all exhibit very similar trends and similar peak temperatures, as shown in Fig. 9. The sample vial with individual PAHs spiked had 100 ng PAH for each TPD run, while the sample vial spiked with 16 PAHs had 500 ng each for a total of 8,000 ng of PAHs for each single TPD run. These differences in PAH mass

concentrations did not result in differences in peak temperature responses.

To visually compare the TPD response from the various solid surfaces studied, the data were normalized by dividing by the total area under the peak of the TPD response curve (for Figs. 10, 11, and 12), which corresponds to the total PAH mass desorbed from the solid. For the pulverized activated carbon, desorption was not complete within the 400°C temperature limit, and peak temperatures could not be assessed. These samples showed the beginning of an apparent peak near the upper temperature limit of 400°C, but since these peaks are not complete, they could not be properly scaled, and are not further discussed. Figure 10 compares the normalized TPD response for PAH molecular weight 228 for the solid surfaces showing complete peaks of desorption. The peak temperature of PAH release for sand is similar to that seen for the glass beads and the

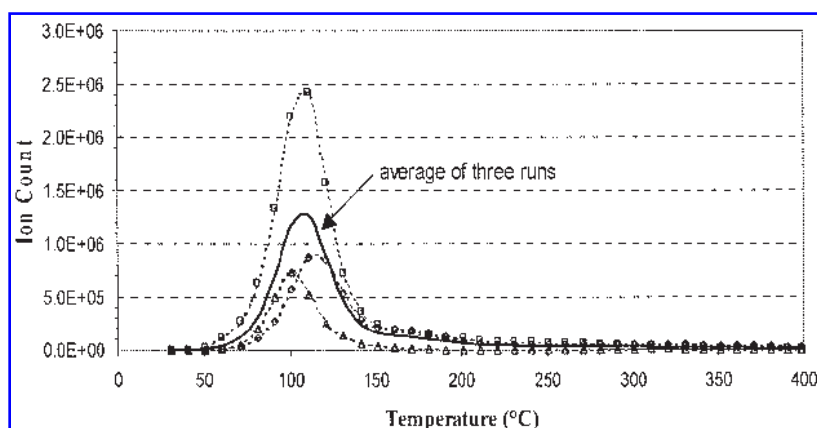


Figure 8. Three thermal program desorption mass spectrometry runs and average response for PAH homolog 252 (benzo[a]pyrene, benzo[b]fluoranthene, and benzo[k]fluoranthene) spiked onto sand at 20 ppm.

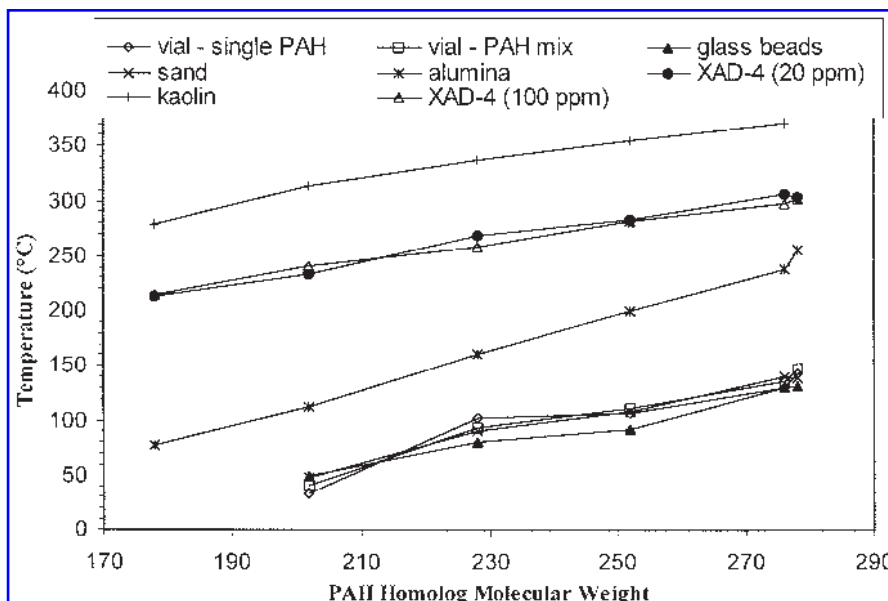


Figure 9. Peak desorption temperatures for PAHs spiked onto different solid surfaces, which illustrates the change in peak temperature for release of PAHs from different solids.

spiked sample vial. The remaining three substrates: alumina, XAD-4, and kaolin show increasing peak temperatures. For molecular weight 228, the peak desorption temperature for sand is 90°C, compared to 161°C for alumina, 265°C for XAD-4, and 338°C for kaolin.

Modeling release of PAHs during TPD

The desorption of PAHs and other hydrophobic organic compounds from solids can be modeled as a first-order rate process as in Equation (3).

$$\frac{dC}{dt} = -kC \tag{3}$$

where C is the concentration of the PAHs present in the solid, k is the rate constant, and t is time. An Arrhenius equation is typically used to describe the change in the rate constant, with temperature as shown in Equation (4).

$$k = \nu e^{-E/RT} \tag{4}$$

where E is the desorption activation energy (J/mol), ν is the preexponential factor (s^{-1}), and R is the universal gas

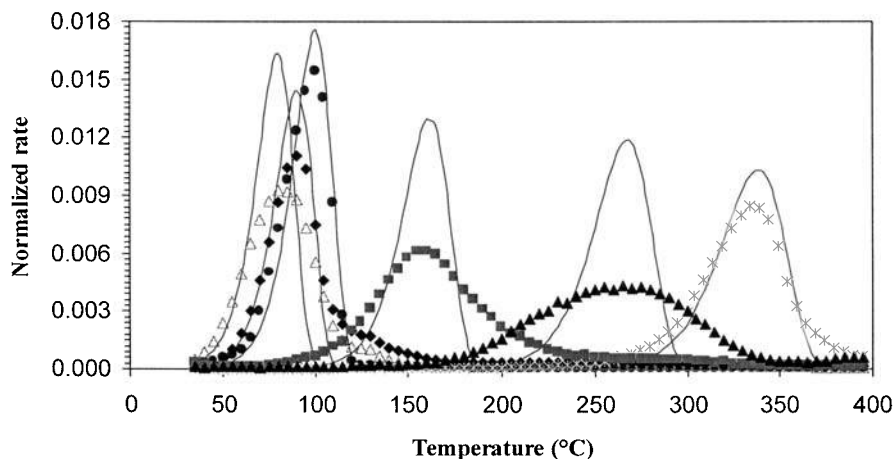


Figure 10. Thermal program desorption mass spectrometry response for MW 228 (benzo[a]anthracene and chrysene) showing release from different solid surfaces and comparison with a model based on parameter estimates using the peak temperature method and assuming $\nu = 10^{13} s^{-1}$.

constant (J/mol-K). Equation (5) is obtained by combining Equations (3) and (4) and replacing dt with dT , assuming a constant rate of temperature rise β (K/s).

$$\frac{dC}{dT} = -\frac{\nu}{\beta} C e^{-E/RT} \quad (5)$$

The form of this equation is similar to expressions used to describe the effect of temperature increase on release of sorbate materials from surfaces. The thermal desorption of compounds from a solid surface is often described in the surface science field by a similar Arrhenius expression known as the Polanyi-Wigner equation (De Jong and Niemantsverdriet, 1990):

$$\frac{d\theta}{dT} = -\nu(\theta)\theta^n e^{-E(\theta)/RT} \quad (6)$$

where θ is the adsorbate coverage (unitless), n is the order of the desorption process, and for which both ν and E can be functions of adsorbate coverage. The Polanyi-Wigner equation expressed in simplified terms results in Equation (5) when the order of the reaction is 1, the heating rate is constant, the terms ν and E are assumed to be coverage independent, and coverage corresponds to concentration. Equation (5) and several modified versions of it have been used extensively in the surface science literature to describe the desorption of gases sorbed on metal surfaces and catalysts (Falconer and Madix, 1975; King, 1975; De Jong and Niemantsverdriet, 1990). Three methods used traditionally in the surface science field to fit the two parameters E and ν in Equation (5) to measured TPD data were evaluated in this work. A fourth method to fit Equation (5) to the measured TPD data was based on a nonlinear curve fitting technique. These four methods are described below.

1. Peak temperature method (Redhead, 1962). In this method, Equation (5) is differentiated to obtain a relationship of E with the peak temperature of desorption for concentration-independent desorption parameters:

$$\frac{E}{RT_p^2} = \frac{\nu}{\beta} e^{-E/RT_p} \quad (7)$$

where T_p is the peak temperature of desorption, and β is the heating rate in K/s. Equation (7) is an implicit function of E , and needs to be solved by iteration. A major shortcoming of this method, however, is that a value of ν has to be assumed to estimate E . Values of ν used in the surface science applications vary widely, anywhere between 10^{10} and 10^{20} s^{-1} (Rudzinski *et al.*, 1997). De Jong and Niemantsverdriet (1990) suggest a typical value of 10^{13} s^{-1} .

2. Chan-Aris-Weinberg method (1978). This method utilizes both the peak temperature and peak width at half or three quarters of the maximum intensity to estimate

the two parameters of the Polanyi-Wigner model. The equations used to estimate the parameters from the peak temperature and peak width at half height are:

$$E = RT_p[-1 + (\gamma^{-2} + 5.832\gamma)^{0.5}] \quad (8)$$

$$\nu = \frac{E\beta}{RT_p^2} e^{E/RT_p} \quad (9)$$

where γ is the ratio of peak temperature (K) and peak width at half height. Using this method, both E and ν can be estimated independently.

3. Leading edge method (Habenschaden and Kuppers, 1984). This method uses the initial part of the TPD curve where it is assumed that the change in surface concentration is small and, therefore, concentration remains constant. This simplifies Equation (5) and a plot of $\ln(dC/dT)$ vs. $1/T$ yields a slope of $-E/R$ and an intercept of $\ln(\nu/\beta)$. A shortcoming of this method is that it uses the leading edge of the thermal desorption spectrum, where the desorption rate is small, and therefore the accuracy of measurement is low.
4. Nonlinear curve fitting. In this method, the two parameters E and ν in Equation (5) are fitted using a nonlinear curve fitting routine by minimizing the sum of squared errors between the model and the measured TPD data. The TPD data obtained in ion counts vs. temperature are first normalized by dividing by the total area under the TPD curve, which corresponds to total release. The TPD curves then are replotted as normalized rate vs. temperature prior to nonlinear curve fitting. The model shown in Equation (5) was solved with an initial normalized concentration of 1 at the beginning of the TPD run. A generalized reduced gradient nonlinear optimization code (Microsoft Excel 97 solver) was used to minimize the sum of squared errors between the model and the data.

Results of model fitting to TPD data

Interpretation of the data by the peak temperature method required an assumption of the parameter ν . An

Table 3. Estimated values of E using the peak temperature method [Equation (7)] for three values of ν . Units are kJ/mol for E and s^{-1} for ν , for PAH homolog 228.

	T_p ($^{\circ}C$) (MW 228)	$\nu = 10^{12}$ E	$\nu = 10^{13}$ E	$\nu = 10^{14}$ E
Sample vial	102	100	106	113
Glass beads	81	94	100	107
Sand	94	96	103	110
Alumina	161	116	124	132
XAD-4	265	145	155	166
Kaolin	338	164	176	187

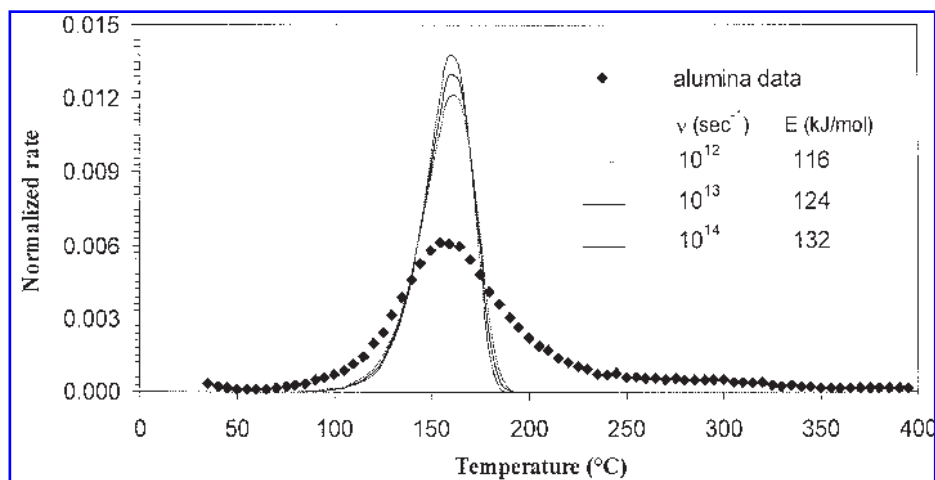


Figure 11. Comparison of model fit using the peak temperature method for three assumed values of preexponential factor ν and corresponding activation energy E for desorption of PAH molecular weight 228 (benzo[a]anthracene and chrysene) from alumina.

average ν value of 10^{13} s^{-1} suggested by De Jong and Niemantsverdriet (1990) was used, as well as assumed values higher by an order of magnitude and lower by one order of magnitude for comparison. The value of E for these three values of ν were estimated by solving Equation (7) iteratively, and the results for PAH molecular weight 228 are shown in Table 3. Figure 10 compares the model prediction of TPD response for PAH molecular weight 228 for six solid surfaces for an assumed value of $\nu = 10^{13} \text{ s}^{-1}$. As may be expected, the fitted model simulation using the parameter values estimated from the peak temperature method match the peak temperatures of the TPD response well, as shown in Fig. 10 for an assumed value of $\nu = 10^{13}$. However, the peak shapes are not predicted well as only the peak temperature information from the TPD response is used in the data analysis. As seen in Table 3, the estimated values of E increases by approximately 15% as the value of ν is

increased from 10^{12} to 10^{14} for each solid material. It is clear that without an independent measure of ν , unique values of the two parameters cannot be estimated by this method. This is illustrated in Fig. 11 where the model simulation using the three estimated values of E for the three assumed values of ν are compared with the TPD data for desorption of molecular weight 228 from alumina. For all three cases, the peak temperature matches closely with the observed data; however, the values of the parameters are quite different.

The estimated values of E and ν using the other three fitting methods are shown in Table 4 for PAH homolog 228. The estimation method based on peak temperature and width (method 2) provides parameter values that are small for both E and ν compared to those estimated by the other three methods. A possible reason for the very different values of the parameters estimated using method 2 is the high sensitivity to the peak width value in the es-

Table 4. Estimated values of E and ν using Chan-Aris-Winberg, leading edge, and nonlinear curve fitting techniques for PAH homolog 228 desorption.

	Chan-Aris-Winberg		Leading edge		Nonlinear fit	
	E	ν	E	ν	E	ν
Sample vial	23	5.39	100	1.55E+12	94	2.00E+11
Glass beads	17	0.87	82	1.46E+10	56	1.50E+06
Sand	22	5.59	117	1.31E+15	76	7.80E+08
Alumina	20	0.63	58	3.08E+04	53	1.10E+04
XAD-4	20	0.13	72	4.38E+04	53	4.10E+02
Kaolin	39	4.67	103	2.19E+06	137	4.20E+09

Units are kJ/mol for E and s^{-1} for ν .

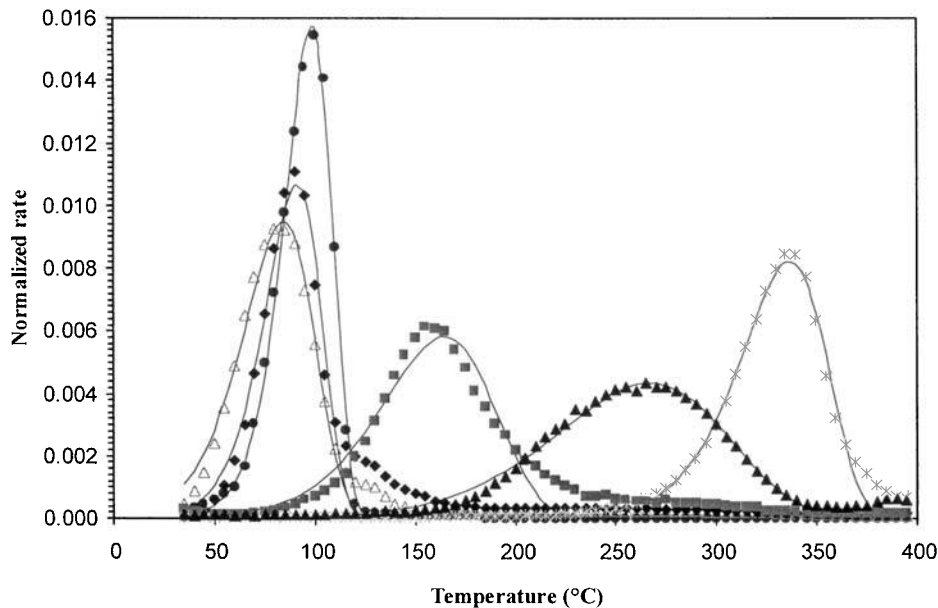


Figure 12. Fitted model to thermal program desorption mass spectrometry data for PAH MW 228 (benzo[a]anthracene and chrysene) for various solids using the nonlinear curve fitting techniques.

timation. PAH molecular weights measured in this research comprise two or more PAH compounds per homolog, as shown in Table 1, and which may result in wider TPD curves than what is expected from a single

compound. As seen in Equations (8) and (9), a smaller value of the ratio of peak temperature to peak width results in the estimation of a smaller value of E and ν . Therefore, the parameter estimation method using the

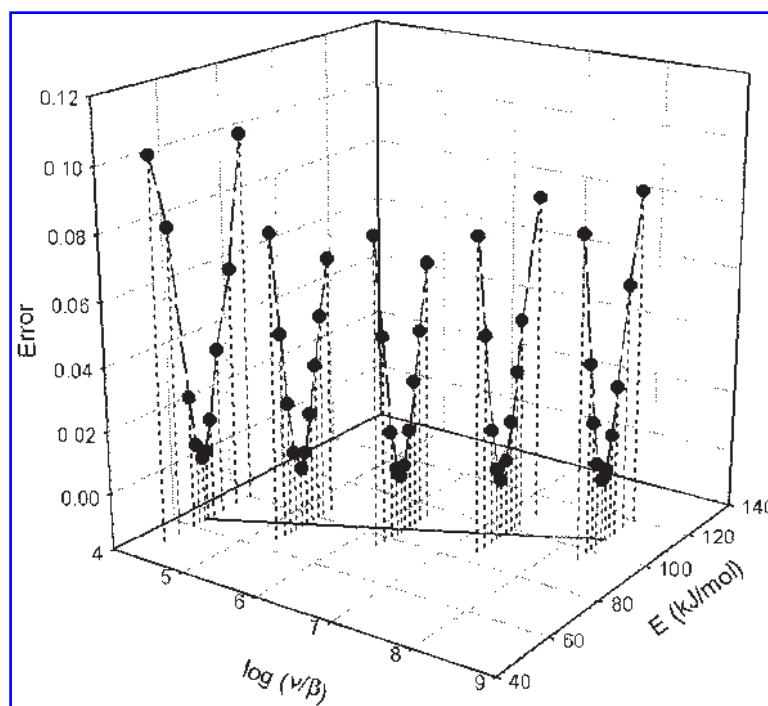


Figure 13. Error surface plot showing a long valley illustrating the difficulty in obtaining a unique set of parameters to describe the thermal program desorption mass spectrometry for release of PAH MW 228 (benzo[a]anthracene and chrysene) from XAD 4.

peak width may not be appropriate for this case. Historically, this method has been used for the thermal programmed desorption of simple organics from clean metal surfaces (Masel, 1996).

The nonlinear curve fitting technique provided the best fit to the entire dataset among the four methods tested as demonstrated in Fig. 12. This method provided a good fit of not just the peak temperature but also the shape of the entire TPD curves.

An inherent problem with all these data reduction methods lies in fact that there is a high degree of correlation between the parameters to be estimated. Correlation between the two parameters E and ν in Equation (5) makes it difficult to estimate a unique set of parameter values by fitting TPD data. Thus, several sets of these parameter values may provide a reasonable description of the measured TPD response. This is illustrated below by analyzing the error space of the parameter fitting.

Parameter estimation and error analysis from nonlinear curve fitting

A sensitivity analysis was performed to investigate the problem associated with estimating unique parameters by fitting the model in Equation (5) to the TPD data. TPD data for PAH molecular weight 228 on XAD-4 was used to perform the sensitivity analysis. For a range of assumed values of the parameter ν/β [K^{-1}] spanning four orders of magnitude, the value of E was varied to span a range across the value that provided a minimum of the sum of squared errors. The sum of squared error values are plotted as a function of ν/β and E as shown in Figure (13). The error surface forms a long, narrow valley with several minimum values as illustrated. Since the two parameters were correlated, several sets of values of ν/β and E provide a good fit and a minimum value of sum of squared errors. These sets of possible parameter values fall in a straight line in the ν/β - E plane. The high correlation between the two model parameters makes their estimation difficult from the TPD data alone and results in the large variability in the parameter values estimated by the different methods.

SORPTION ON MINERAL AND ORGANIC SURFACES

In the measurements presented of the TPD response from spiked materials, each compound was spiked at 20 ppm by mass that is a 2.0×10^{-5} gram of compound per gram of material. The surface coverages for the sand, alumina, kaolin, XAD-4, were estimated assuming a planar orientation for chrysene with planar width of 8 angstroms and length of 13.9 angstroms (NIST Standard Reference Data,

<http://ois.nist.gov/pah>), giving a saturated coverage ($\theta = 1$) monolayer specific surface of 3.0×10^3 m^2/g of compound.

The surface area coverage corresponding to 20 ppm chrysene are listed in Table 5. Sorption mechanisms on XAD (a polymer) is likely very different than on mineral surfaces. Inspection of Table 5 for mineral surfaces holds the trend of increasing T_p with decreasing surface coverage. In their thermal desorption study, Choren *et al.* (1997) report that alumina exhibited greater affinity than silica particularly for compounds with π bonds. Both studies suggest that surface chemistry plays a key role in the availability of these compounds.

CONCLUSIONS

This technique of using TPD results to estimate relative desorption rate constants provides a method to compare the relative strength of PAH binding to different solid surfaces, and these data may give an indication of reduced PAH availability when sorbed to these surfaces. Overall, the results give evidence for changes in the relative temperature and rate of release (for a given mass homolog of PAH) from different types of solids under vapor phase conditions. This work is a demonstration that thermal desorption is a potentially useful qualitative tool for judging the "relative" tenacity of vapor-phase (non-water-wet) adsorption in some systems, and an exploration of crosscorrelation among some existing model approaches. However, quantitative estimates of the desorption rate constants at ambient temperatures, or apparent binding energies, are not currently feasible from TPD analysis alone due to the problem associated with determining an unique set of parameters in a two-parameter model. Thus, for assessment of binding energies for sorbed PAHs, and the effect of temperature of PAH release from solids, an independent measurement of the desorption rate at a fixed temperature is required in combination with thermal programmed desorption. This is the focus of a subsequent investigation.

Table 5. Sorption properties for PAH homolog 228.

	Specific area ^a (m^2/g)	Coverage q (at 20 ppm)	T_p ($^{\circ}C$) (MW 228)
Sand	0.01	>1	94
Alumina	3.7	0.016	161
XAD-4	760	0.000079	265
Kaolin	23	0.0026	338

^aSpecific area using BET nitrogen test.

ACKNOWLEDGMENTS

Funding and technical support for this research was obtained from the Department of Defense through the Strategic Environmental Research and Development Program (SERDP) and the U.S. Army Engineer Research Development Center (ERDC).

REFERENCES

- CHAN, C.M., ARIS, R., and WEINBERG, W.H. (1978). An analysis of thermal desorption mass spectra. *Appl. Surf. Sci.* **1**, 360.
- CHOREN, E., MORONTA, A., VARELA, G., ARTEAGA, A., and SANCHEZ, J. (1997). Condensation of olefins on clays. Gas-solid systems. Part I. Gravimetric methods. *Clays Clay Minerals* **45**, 213.
- DE JONG, A.M., and NIEMANTSVERDRIET, J.W. (1990). Thermal desorption analysis: Comparative test of ten commonly applied procedures. *Surf. Sci.* **233**, 355.
- FALCONER, J.L., and MADIX, R.J. (1975). Flash desorption activation energies. Formic acid decomposition and carbon monoxide desorption from nickel (110). *Surf. Sci.* **48**, 393.
- FARRELL, J., GRASSIAN, D., and JONES, M. (1999). Investigation of mechanisms contributing to slow desorption of hydrophobic organic compounds from mineral solids. *Environ. Sci. Technol.* **33**, 1237.
- GHOSH, U., GILLETTE, J.S., LUTHY, R.G., and ZARE, R.N. (2000). Microscale location, characterization, and association of polycyclic aromatic hydrocarbons on harbor sediment particles. *Environ. Sci. Technol.* **34**, 1729.
- GHOSH, U., TALLEY, J.W., and LUTHY, R.G. (2001). Particle-scale investigation of PAH desorption kinetics and thermodynamics from sediment. *Environ. Sci. Technol.* **35**, 3468.
- HABENSCHADEN, E., and KUPPERS, J. (1984). Evaluation of flash desorption spectra. II. *Surf. Sci.* **138**, L147.
- KARAPANAGIOTA, H.K., KLEINEIDAM, S., SABATINI, D.A., GRATHWOHL, P., and LIGOUIS, B. (2000). Impacts of heterogeneous organic matter on phenanthrene sorption: Equilibrium and kinetic studies with aquifer material. *Environ. Sci. Technol.* **34**, 406.
- KEYS, B.R., and SILCOX, G.D. (1994). Fundamental study of the thermal desorption of toluene from montmorillonite clay particles. *Environ. Sci. Technol.* **28**, 840.
- KING, D.A. (1975). Thermal desorption from metal surfaces. *Surf. Sci.* **47**, 384.
- LUTHY, R.G., AIKEN, G.R., BRUSSEAU, M.L., CUNNINGHAM, S.D., GSCHWEND, P.M., PIGNATELLO, J.J., REINHARD, M., TRAINA, S.J., WEBER, W.J., JR., and WESTALL, J.C. (1997). Sequestration of hydrophobic organic contaminants by geosorbents. *Environ. Sci. Technol.* **31**, 3341.
- MACKAY, D., BOBRA, A., CHAN, D.W., and SHIU, W.Y. (1982). Vapor-pressure correlations for low-volatility environmental chemicals. *Environ. Sci. Technol.* **16**, 645.
- MACKAY, D., SHIU, W.Y., and MA, K.C. (1992). *Illustrated Handbook of Physical-Chemical Properties and Environmental Fate for Organic Chemicals*. Chelsea: Lewis Publishers.
- MASEL, R.I. (1996). *Principles of Adsorption and Reaction on Solid Surfaces*. New York: John Wiley & Sons.
- OJA, V., and SUUBERG, E.M. (1997). Development of a non-isothermal Knudsen effusion method and application to PAH and cellulose tar vapor pressure measurement. *Anal. Chem.* **69**, 4619.
- PRAUSNITZ, J.M. (1969). *Molecular Thermodynamics of Fluid-Phase Equilibria*. Englewood Cliffs, NJ: Prentice Hall.
- REDHEAD, P.A. (1962). Thermal desorption of gases. *Vacuum* **12**, 203.
- ROBBAT, A., JR., LIU, T., and ABRAHAM, B.M. (1992). Evaluation of a thermal desorption gas chromatograph/mass spectrometer: On-site detection of polychlorinated biphenyls at a hazardous waste site. *Anal. Chem.* **64**, 358.
- RUDZINSKI, W., STEELE, W.A., and ZARABLICH, G. (1997). *Equilibria and Dynamics of Gas Adsorption on Heterogeneous Solid Surfaces*. New York: Elsevier Press.
- SCHWARZENBACH, R.P., GSCHWEND, P.M., and IMBODEN, D.M. (1993). *Environmental Organic Chemistry*. New York: John Wiley and Sons.
- TESCONI, M., and YALKOWSKI, S.H. (1998). A novel thermogravimetric method for estimating the saturated vapor pressure of low-volatility compounds. *J. Pharmaceut. Sci.* **87**, 1512.
- WEAST, R.C. (1985). *CRC Handbook of Chemistry and Physics*. Boca Raton, FL: CRC Press.
- YUN, Y., and MEUZELAAR, H.L.C. (1991). Vacuum pyrolysis mass spectrometry of Pittsburgh No. 8 coal: Comparison of three different, time-resolved techniques. *Energy Fuels* **5**, 22.